

Nonlinear optical response of truly chiral phonons: Light-induced phonon angular momentum, Peltier effect, and orbital current

Hiroaki Ishizuka¹ and Masahiro Sato²

¹*Department of Physics, Institute of Science Tokyo, Meguro, Tokyo, 152-8551, Japan*

²*Department of Physics, Chiba University, Chiba 263-8522, Japan*

(Dated: May 9, 2025)

The nonlinear optical responses of chiral phonons to terahertz and infrared light are studied using the nonlinear response theory. We show that the photo-induced angular momentum increases with the square of the chiral-phonon relaxation time τ , giving a significantly larger angular momentum compared to ordinary phonons. We also find that the photo-induced Peltier effect by chiral phonons occurs through a mechanism distinct from those proposed recently; the induced energy current scales $\propto \tau^2$, giving a larger energy current in the clean limit. We prove a linear relation between the generated angular momentum and the energy current. Lastly, we show that the orbital current, an analog of the spin current, occurs through a nonlinear response. These findings demonstrate the unique properties and functionalities of chiral phonons.

PACS numbers:

Introduction — Chiral phonon is a phonon mode whose angular momentum and the wavenumber couples, $\mathbf{L} \cdot \mathbf{k} \neq 0$, where \mathbf{L} is the crystal angular momentum and \mathbf{k} is the momentum of phonons, respectively [1]. In chiral crystals, the degeneracy of chiral phonons is lifted, and the modes possess a non-zero group velocity at the symmetric points in the Brillouin zone [Fig. 1(b)] [2]. The coupling of the group velocity and the chirality allows small-momentum phonons to carry energy and angular momentum efficiently, providing unique properties and making them attractive for applications.

In studying phonons and exploring their functionalities, the optical response has played a central role. For example, Raman scattering techniques were used to study truly chiral phonons [1], and optical generation of phonon angular momentum and related phenomena were studied in several materials [3–12]. As demonstrated by these works, unlike phononic heat conduction and thermal Hall effect [13–20], which are often dominated by acoustic gapless phonons, optical techniques are especially useful for studying and utilizing optical gapped phonons. On the other hand, recent studies on the photocurrent of electrons revealed intriguing features, such as non-local current transport [21, 22], robustness against disorder [23–25], and the generation of spin [26] and orbital [27] photocurrents. Similar phenomena in magnetic excitations [28–32] and phonons [33] were theoretically predicted. Chiral phonons have properties distinct from the models used in these studies, possibly realizing unique nonlinear responses.

To understand the optical properties of chiral phonons, we study a series of second-order nonlinear responses to terahertz and infrared light: Angular momentum generation, photo-induced nonlinear Peltier effect, and orbital current. For the angular momentum generation and photo-induced Peltier effect, we find that a mechanism unique to the chiral phonons induces a larger response than that in non-chiral phonons. The angular momentum and phonon

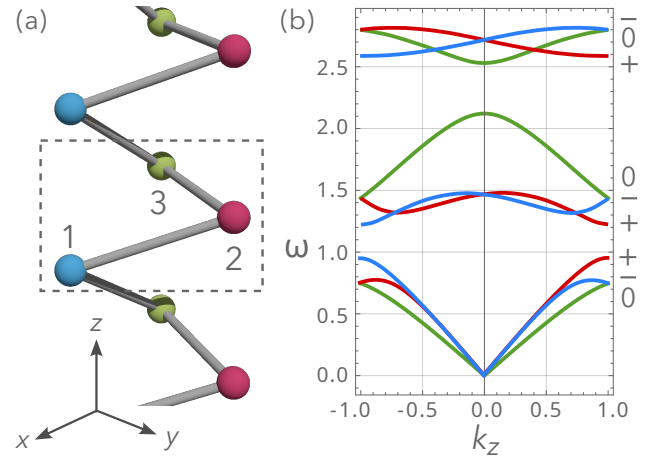


FIG. 1. (a) Schematic of Te-like three-ion model. The dashed box indicates the unit cell. (b) The phonon dispersion of Te-like model. The red, green, and blue curves are the bands with crystal angular momentum $L^z = 1, 0, \text{ and } -1$, respectively.

photocurrent induced by this mechanism are polarization-dependent, distinct from those induced by linearly polarized light. In addition, we argue that an orbital photocurrent of phonons occurs in chiral materials, which might be functional for spintronics applications.

Chiral phonon — An example of the model with truly-chiral phonon modes and its dispersion are shown in Fig. 1 [34]. The model is an one-dimensional atom chain consisting of a lattice with three ions in a unit cell forming a spiral structure. The Hamiltonian reads,

$$\hat{H}_{CP} = \sum_{ia\mu} \frac{\hat{p}_{ia\mu}^2}{2m_a} + \frac{1}{2} \sum_{(ia\mu, jb\nu)} (\hat{u}_{ia\mu} - \hat{u}_{jb\nu}) D_{ia\mu, jb\nu} (\hat{u}_{ia\mu} - \hat{u}_{jb\nu}), \quad (1)$$

where $D_{ia\mu,jb\nu}$ is the dynamical matrix, $\hat{u}_{ia\mu}$ is the displacement along the μ axis of a ($= 1, 2, 3$) sublattice atom in i th unit cell, and $p_{ia\mu}$ is the conjugate momentum of $\hat{u}_{ia\mu}$ satisfying $[\hat{u}_{ia\mu}, \hat{p}_{jb\nu}] = i\delta_{ij}\delta_{ab}\delta_{\mu\nu}$; here we set the Dirac constant $\hbar = 1$ and the sum is over all pairs of $ia\mu$. The dynamical matrix is $D_{i-13\mu,i1\nu} = (D_{31})_{\mu\nu}$ where

$$D_{31} = \begin{pmatrix} K_{11} & 0 & 0 \\ 0 & K_{22} & -\Delta K \\ 0 & -\Delta K & K_{33} \end{pmatrix}, \quad (2)$$

for the nearest-neighbor bonds between $a = 1$ and 3 sublattices, and the nearest-neighbor matrices for the other two bonds are given by D_{31} rotated by 120° . Here, K_{ii} ($i = 1, 2, 3$) and ΔK are the stiffness constants [34].

The phonon bands in Fig. 1(b) are characterized by the crystal angular momentum of ions [34]; the phonon bands with non-zero crystal angular momentum are called chiral phonons. A unique feature of truly chiral phonons is the linear crossing of phonon bands at the symmetric point [Γ in the case of Fig. 1(b)]. The crossing of two phonon bands results from different angular momentum, which prohibits the anti-crossing. In the below, we focus on doubly degenerate cases in which only two bands cross at $\mathbf{k} = \mathbf{0}$.

Nonlinear response theory — To study the second-order dc response of quantum phonons to electromagnetic waves, we start by considering non-interacting phonon models with n_{ph} phonon bands. The Hamiltonian is given by

$$\hat{H} = \sum_{\mathbf{k}, n} \omega_{n\mathbf{k}} (\hat{b}_{n\mathbf{k}}^\dagger \hat{b}_{n\mathbf{k}} + \frac{1}{2}), \quad (3)$$

and the light-matter coupling,

$$\hat{H}' = \sum_{\mu, n, \mathbf{k}} [\beta_{n\mathbf{k}}^\mu \hat{b}_{n\mathbf{k}} + (\beta_{n\mathbf{k}}^\mu)^* \hat{b}_{n\mathbf{k}}^\dagger] E_\mu(t), \quad (4)$$

with $\beta_{n\mathbf{k}}^\mu$ being the coupling constant and $E^\mu(t)$ is the external field. Here, $\hat{b}_{n\mathbf{k}}$ ($\hat{b}_{n\mathbf{k}}^\dagger$) is the annihilation (creation) operator of a phonon with band index n and momentum \mathbf{k} , and $\omega_{n\mathbf{k}}$ ($\omega_{n\mathbf{k}} \leq \omega_{m\mathbf{k}}$ if $n < m$) is its phonon frequency. The observables we study in this work are assumed to be

$$\begin{aligned} \hat{O}_\lambda = & \sum_{n, m, \mathbf{k}} \hat{b}_{n\mathbf{k}}^\dagger o_{nm}^\lambda(\mathbf{k}) \hat{b}_{m\mathbf{k}} + \hat{b}_{n\mathbf{k}}^\dagger o_{\bar{n}\bar{m}}^\lambda(\mathbf{k}) \hat{b}_{\bar{m}-\mathbf{k}} \\ & + \hat{b}_{n-\mathbf{k}} o_{\bar{n}\bar{m}}^\lambda(\mathbf{k}) \hat{b}_{m\mathbf{k}} + \hat{b}_{n-\mathbf{k}} o_{\bar{n}\bar{m}}^\lambda(\mathbf{k}) \hat{b}_{\bar{m}-\mathbf{k}}. \end{aligned} \quad (5)$$

The general formula of the nonlinear response tensor $\chi_{\lambda;\mu\nu}(\Omega; \omega, \Omega - \omega)$ for phonons are given recently [33], which is also summarized in the supplemental material [35]. Here, Ω and ω ($-\omega$) are, respectively, the frequencies of the observable and the μ (ν) component of the applied wave.

For the case of the direct coupling between the ion charge and a uniform electric field, which we focus on, $\beta_{n\mathbf{k}}^\mu$ reads

$$\beta_{n\mathbf{0}}^\mu = \sum_a q_a |n\mathbf{0}\rangle_{a\mu} \sqrt{\frac{N}{2m_a \omega_{n\mathbf{0}}}}, \quad (6)$$

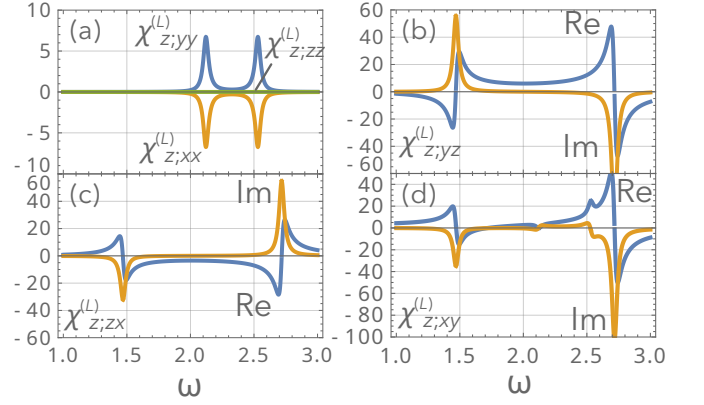


FIG. 2. (a) Real part of the nonlinear susceptibility $\chi_{z;xx}^{(L)}(0; \omega, -\omega)$, $\chi_{z;yy}^{(L)}(0; \omega, -\omega)$, and $\chi_{z;zz}^{(L)}(0; \omega, -\omega)$, and the frequency dependence of (b) $\chi_{z;yz}^{(L)}(0; \omega, -\omega)$, (c) $\chi_{z;zx}^{(L)}(0; \omega, -\omega)$, and (d) $\chi_{z;xy}^{(L)}(0; \omega, -\omega)$ for the Te-like model. The results are for $\delta = 0.23$, $K_1 = 3/2$, $K_2 = 1/2$, $K_3 = 3$, $\theta = 0.3\pi$, $a = 1$, $c = 1$, $m = 1$, $q_1 = 0$, $q_2 = 1$, $q_3 = -1$, and $\tau = 20$.

and $\beta_{n\mathbf{k}}^\mu = 0$ for $\mathbf{k} \neq \mathbf{0}$. Here, N is the number of unit cells, $|n\mathbf{k}\rangle$ is the n th eigenstate of dynamical matrix with the wavenumber \mathbf{k} , and q_a is the charge of ions on the a th sublattice.

Phonon angular momentum — Using the equilibrium position of ion $r_{ia\mu}^0 = r_{ia\mu} - u_{ia\mu}$ where $r_{ia\mu}$ is the position of the atom, the angular momentum of a lattice reads $\mathbf{L}^{\text{atm}} = \sum_{ia} \mathbf{r}_{ia} \times \mathbf{p}_{ia} = \mathbf{L}^{\text{lat}} + \mathbf{L}^{\text{ph}}$ where $\mathbf{L}^{\text{lat}} = \sum_{ia} \mathbf{r}_{ia}^0 \times \mathbf{p}_{ia}$ is the lattice angular momentum and $\mathbf{L}^{\text{ph}} = \sum_{ia} \mathbf{u}_{ia} \times \mathbf{p}_{ia}$ is the phonon angular momentum. The z component of the phonon (crystal) angular momentum is given by Eq. (5), where $o_{nm}^\lambda(\mathbf{k})$ is replaced by $M_{nm}(\mathbf{k}) = \frac{1}{4} \frac{\omega_{m\mathbf{k}} + \omega_{n\mathbf{k}}}{\sqrt{\omega_{n\mathbf{k}} \omega_{m\mathbf{k}}}} \langle n\mathbf{k} | M^z | m\mathbf{k} \rangle = -M_{\bar{n}\bar{m}}(\mathbf{k})$ and $M_{\bar{n}\bar{m}}(\mathbf{k}) = -\frac{1}{4} \frac{\omega_{n\mathbf{k}} - \omega_{m\mathbf{k}}}{\sqrt{\omega_{n\mathbf{k}} \omega_{m\mathbf{k}}}} \langle n\mathbf{k} | M^z | m\mathbf{k} \rangle = -M_{n\bar{m}}(\mathbf{k})$ [35–38]. Here, M^z is a matrix whose elements are $(M^\lambda)_{a\mu, b\nu} = -i\delta_{ab}\epsilon_{\lambda\mu\nu}$, where δ_{ab} is the Kronecker's delta and $\epsilon_{\mu\nu\lambda}$ is the Levi-Civita tensor.

In view of the optical responses, the phonon angular momentum generated by light irradiation can be described as a second-order dc response. The ω dependence of the nonlinear response tensor $\chi_{\lambda;\mu\nu}^{(L)}(0; \omega, -\omega)$ for the angular momentum is shown in Fig. 2. In Figs. 2(b), the two peaks of $\text{Im}[\chi_{z;xy}^{(2)}(0; \omega, -\omega)]$ at $\omega \simeq 1.47$ and 2.72 , which correspond to the frequencies of $\mathbf{k} = \mathbf{0}$ chiral phonons in Fig. 1(b), indicate that the angular momentum of phonons is generated by exciting chiral phonons with circularly polarized light. This is consistent with the intuition that circularly polarized light induces the circular motion of atoms. Figures 2(b) and 2(c) also show that the angular momentum is generated by the circularly polarized electric field in the yz and zx planes. The results indicate that angular momentum can be induced with circularly polarized light

regardless of the incident direction in the Te-like model.

We note that the height of the peaks at the chiral phonon frequencies increases $\text{Im}[\chi_{z;\mu\nu}^{(L)}(0; \omega, -\omega)] \propto \tau^2$ in the long τ limit, unlike the usual resonance peaks that increase as τ^1 . The peaks for polarization-dependent angular momentum appears from the $\omega_{n\mathbf{0}} = \omega_{m\mathbf{0}}$ terms in the general formula (Eq. (??) in [35]), which reads

$$\chi_{\lambda;\mu\nu}^{(L)} \sim \frac{2\tau}{\pi V} \sum_{\alpha, \beta}^{N_n} \frac{\beta_{n\alpha\mathbf{0}}^\mu \Im[M_{n\alpha, n\beta}(\mathbf{0})](\beta_{n\beta\mathbf{0}}^\nu)^*}{\omega - \omega_{n\mathbf{0}} - \frac{i}{2\tau}}, \quad (7)$$

around $\omega = \omega_{n\mathbf{0}}$. Here, we relabeled the bands by a pair of indexes $n\alpha$, where n is for different energy levels $\omega_n(\mathbf{0})$ and α is the index for N_n degenerate bands with frequency $\omega_n(\mathbf{0})$. The equation shows that the height of the peak increases $\propto \tau^2$. In addition, for the quadratic phonon models in Eq. (1), one can take the eigenstates as $|n\alpha\mathbf{k}\rangle = |n\alpha, -\mathbf{k}\rangle^*$, in which case the coefficients of the angular momentum operator satisfies $M_{n\alpha, m\beta}(\mathbf{k}) = M_{m\beta, n\alpha}^*(-\mathbf{k}) = -M_{m\beta, n\alpha}(-\mathbf{k})$; in addition, $\beta_{n\alpha\mathbf{0}}^\nu$ in Eq. (6) becomes a real number. Combined with hermiticity, $M_{n\alpha, m\beta}(\mathbf{k}) = M_{m\beta, n\alpha}^*(\mathbf{k})$, the above equality gives $M_{n\alpha, n\alpha}(\mathbf{0}) = 0$ and $M_{n\alpha, n\beta}(\mathbf{0})$ purely imaginary for $\alpha \neq \beta$, indicating that the τ^2 peaks appear only if the degenerate bands exist and that the τ^2 response is dependent on polarization.

The τ^2 dependence suggests that these contributions show behaviors distinct from the well-known resonance phenomena. For instance, they (the τ^2 terms) may dominate the nonlinear response to electromagnetic waves in a material with a long lifetime, realizing a large phonon angular momentum. Such a situation is likely for phonons, whose lifetime is typically longer than that of electronic and magnetic excitations. As chiral phonons, not limited to truly chiral phonons, are degenerate at symmetric points, the τ^2 dependence may explain the large angular momentum [8].

In the last, as shown in Fig. 2(a), we note that a finite angular momentum can also be induced by linearly-polarized light. In the figure, two peaks appear in $\chi_{z;xx}^{(L)}$ and $\chi_{z;yy}^{(L)}$ at $\omega = 2.12$ and 2.53 , the frequencies corresponding to non-chiral phonons ($L_z^{\text{ph}} = 0$ phonons). However, the peaks of the response function increase as $\propto \tau^1$ for these non-chiral phonons. Generating angular momentum using linearly polarized light may appeal to the generation of phonon angular momentum with low-frequency phonons, at which frequency generating a high-intensity circularly polarized light is challenging.

Peltier effect of phonons — Another characteristic of truly chiral phonons is the non-zero group velocity at $\mathbf{k} = \mathbf{0}$ [2], facilitating efficient phonon transport. An interesting phenomenon in this context is the optical Peltier effect of phonons [33], which is a temperature gradient induced by a photocurrent of phonons. The coefficient for the Peltier effect, $\Pi_{\lambda;\mu\nu}(0; \omega, -\omega)$, is calculated by replacing o^λ with the phonon energy

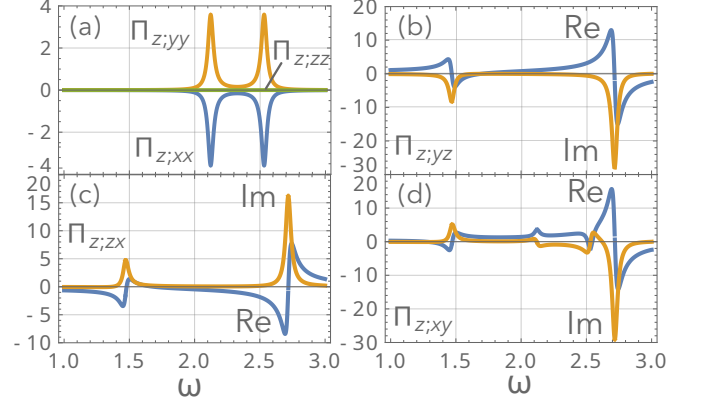


FIG. 3. Real part of the Peltier coefficient for (a) $\Pi_{z;xx}(0; \omega, -\omega)$, $\Pi_{z;yy}(0; \omega, -\omega)$, and $\Pi_{z;zz}(0; \omega, -\omega)$, and the frequency dependence of (b) $\Pi_{z;yz}(0; \omega, -\omega)$, (c) $\Pi_{z;zx}(0; \omega, -\omega)$, and (d) $\Pi_{z;xy}(0; \omega, -\omega)$ for the Te-like model. The results are for $\delta = 0.23$, $K_1 = 3/2$, $K_2 = 1/2$, $K_3 = 3$, $\theta = 0.3\pi$, $a = 1$, $c = 1$, $m = 1$, $q_1 = 0$, $q_2 = 1$, $q_3 = -1$, and $\tau = 20$.

current operator [39], $J_{nm}^\lambda(\mathbf{k}) = \frac{\omega_{n\mathbf{k}} + \omega_{m\mathbf{k}}}{2} v_{nm}^\lambda(\mathbf{k})$, $J_{n\bar{m}}^\lambda(\mathbf{k}) = \frac{\omega_{n\mathbf{k}} - \omega_{m\mathbf{k}}}{2} v_{nm}^\lambda(\mathbf{k})$, $J_{\bar{n}m}^\lambda(\mathbf{k}) = -J_{nm}^\lambda(\mathbf{k})$, $J_{\bar{n}\bar{m}}^\lambda(\mathbf{k}) = -J_{n\bar{m}}^\lambda(\mathbf{k})$, where $v_{nm}^\lambda(\mathbf{k}) = \frac{\langle n\mathbf{k} | \partial_{k_\lambda} \tilde{A}(\mathbf{k}) | m\mathbf{k} \rangle}{4\sqrt{\omega_{n\mathbf{k}}\omega_{m\mathbf{k}}}}$

is the phonon velocity operator with $\tilde{A}_{a\mu, b\nu}(\mathbf{k}) = \sum_i \frac{A_{ia\mu, ob\nu}}{\sqrt{m_a m_b}} e^{-i\mathbf{k} \cdot (\mathbf{r}_{ia} - \mathbf{r}_{ob})}$. Here, we expressed the Hamiltonian in the form $H_{CP} = \frac{1}{2} \sum_{ia\mu, jbv} A_{ia\mu, jbv} u_{ia\mu} u_{jbv}$ for the sake of conciseness [33, 39]; $A_{ia\mu, jbv}$ are $A_{ia\mu, ia\mu} = \sum_{jbv} D_{ia\mu, jbv}$ and $A_{ia\mu, jbv} = -D_{ia\mu, jbv}$ for the Hamiltonian in Eq. (1).

Figure 3 shows the ω dependence of the Peltier coefficient for the Te-like model. The resonance peaks for $\Pi_{z;xx}$ and $\Pi_{z;yy}$ appear at the frequencies for the non-chiral phonons as shown in Fig. 3(a), similar to those in a previous work [33]. In contrast, the resonance peaks appear in the imaginary part for the chiral phonons, $\omega \simeq 1.47$ and 2.72 ; they indicate that a polarization-dependent Peltier effect occurs with circularly polarized light [Figs. 3(b)-3(d)].

To further investigate the nature of the polarization-dependent Peltier effect, we look into the general formula (Eq. (??)) assuming a uniform external field, i.e., $\beta_{n\mathbf{k}}^\mu = 0$ for $\mathbf{k} \neq \mathbf{0}$. Similar to the case of angular momentum, $\Pi_{\lambda;\mu\nu}$ near the resonance frequency, $\omega = \omega_{n\mathbf{0}}$, reads

$$\Pi_{\lambda;\mu\nu} \sim \frac{2\tau}{\pi V} \sum_{\sigma, \sigma'}^{N_n} \frac{\beta_{n\sigma\mathbf{0}}^\mu \Im[v_{n\sigma, n\sigma'}^\lambda(\mathbf{0})](\beta_{n\sigma'\mathbf{0}}^\nu)^*}{\omega - \omega_{n\mathbf{0}} - \frac{i}{2\tau}}. \quad (8)$$

In addition, $v_{n\sigma, m\sigma'}^\lambda(\mathbf{k}) = v_{m\sigma', n\sigma}^\lambda(-\mathbf{k}) = -v_{m\sigma', n\sigma}^\lambda(-\mathbf{k})$ and $v_{n\sigma m\sigma'}^\lambda(\mathbf{k}) = v_{m\sigma' n\sigma}^\lambda(-\mathbf{k})$ holds for an eigenstate basis that satisfies $|n\sigma\mathbf{k}\rangle = |n\sigma, -\mathbf{k}\rangle^*$; the property also holds for the photo-induced angular momentum. Hence, as in the case of the angular momentum, only the degenerate phonon bands contribute to the polarization-dependent Peltier effect.

Equation (8) also shows that the τ dependence of the peak height scales as $\Pi \propto \tau^2$ in the large τ limit, which dependence is distinct from the relation $\Pi \propto \tau$ for the linearly polarized light [33]. Therefore, for a clean material at low temperatures, the polarization-dependent Peltier effect should be larger. The different τ dependence arises from the property of $v_{n\sigma,m\sigma'}^\lambda(\mathbf{k})$ discussed in the previous paragraph, which gives $v_{n,n}^\lambda(\mathbf{0}) = 0$. Hence, the leading order term in Eq. (8) vanishes and the subleading contribution with τ^1 dependence becomes the dominant contribution.

The difference in τ dependence resembles that of the shift and injection currents in photovoltaics [40, 41], and the spin current by two-magnon processes [29]. However, we note that the τ dependence is τ^0 and τ^1 for shift and injection currents, respectively. This power-law difference arises from the absence of the integral over \mathbf{k} in the photocurrent. In the case of photovoltaic effects, an integral over the momentum exists as the current occurs through the excitation of electrons with an arbitrary momentum in the Brillouin zone. In such a case, the integral transforms the Lorentzian in the denominator of Eq. (8) into a constant, reducing the order of τ by one. From Eq. (8), one can also see that the Peltier effect is related to the group velocity of the degenerate bands [35], whereas the Peltier effect by the linearly polarized light is related to the Berry connection of phonons [33]. The close resemblance of the Peltier effect to the photovoltaics implies that the polarization-dependent Peltier effect is essentially the injection current of phonons.

For further discussion, we focus on the doubly degenerate case as in the Te-like model. In this case, the equality below Eq. (8) indicates that $v_{n\alpha,n\beta}^\lambda(\mathbf{0}) = \bar{v}_n^\lambda (\sigma^y)_{\alpha\beta}$ where \bar{v}_n^λ is a real constant; note that the same relation holds for the phonon angular momentum, $(L_z^{\text{ph}})_{n\alpha,n\beta} = \bar{L}_{zn}^{\text{ph}} (\sigma^y)_{\alpha\beta}$, where \bar{L}_{zn}^{ph} is a real constant. The proportionality of operators for phonon energy current and angular momentum indicates $\Pi_{\lambda;\mu\nu}(0; \omega, -\omega) \propto \chi_{\lambda;\mu\nu}^{(L)}(0; \omega, -\omega)$ near the resonance frequency $\omega = \omega_n(\mathbf{0})$. Namely, there is a direct relation between the polarization-dependent Peltier effect and the angular momentum of chiral phonons.

Orbital photocurrent — The simultaneous induction of angular momentum and the Peltier effect implies that an orbital current of phonons also occurs. Here, the orbital current refers to the current of phonon angular momentum, analogous to the spin current of electrons. Intuitively, it is a counter flow of phonons with positive and negative angular momentum.

To study the orbital current, we define the orbital current operator J_λ^{orb} from the continuity equation, from which the orbital current and torque terms are defined [35]. The formula is in the form of Eq. (5) with o^λ being

$$v_{nm}^{L\lambda}(\mathbf{k}) = \frac{\langle \mathbf{k}n | M^z \partial_{k_\nu} \tilde{A}_{a\lambda,b\sigma}(\mathbf{k}) | \mathbf{k}m \rangle}{4\sqrt{\omega_{\mathbf{k}n}\omega_{\mathbf{k}m}}} - \frac{\langle \mathbf{k}n | (M^z \tilde{I}^\nu - \tilde{I}^\nu M^z) | \mathbf{k}m \rangle}{8\sqrt{\omega_{\mathbf{k}n}\omega_{\mathbf{k}m}}}, \quad (9)$$

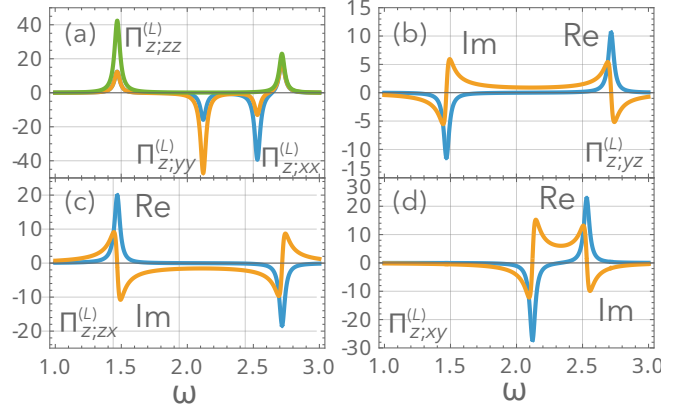


FIG. 4. (a) Real part of the orbital current conductivity $\Pi_{z;zx}^{(L)}(0; \omega, -\omega)$, $\Pi_{z;yy}^{(L)}(0; \omega, -\omega)$, and $\Pi_{z;xx}^{(L)}(0; \omega, -\omega)$, and the frequency dependence of (b) $\Pi_{z;yz}^{(L)}(0; \omega, -\omega)$, (c) $\Pi_{z;zx}^{(L)}(0; \omega, -\omega)$, and (d) $\Pi_{z;xy}^{(L)}(0; \omega, -\omega)$ for the Te-like model. The results are for $\delta = 0.23$, $K_1 = 3/2$, $K_2 = 1/2$, $K_3 = 3$, $\theta = 0.3\pi$, $a = 1$, $c = 1$, $m = 1$, $q_1 = 0$, $q_2 = 1$, $q_3 = -1$, and $\tau = 20$.

and $v_{nm}^{L\lambda}(\mathbf{k}) = v_{nm}^{L\lambda}(\mathbf{k}) = v_{nm}^{L\lambda}(\mathbf{k}) = v_{nm}^{L\lambda}(\mathbf{k})$, where $\tilde{I}_{a\lambda,b\sigma}^\nu = \frac{\delta_{ab}}{m_a} \sum_c \partial_{k_\nu} A_{a\lambda,c\sigma}(\mathbf{k})|_{\mathbf{k}=\mathbf{0}}$. The numerator of Eq. (9) is the product of the angular momentum and the phonon velocity, consistent with the physical intuition. Orbital current generation is studied by combining the nonlinear response theory and Eq. (9).

The calculated conductivities of the nonlinear orbital current $\Pi_{\lambda;\mu\nu}^{(L)}(0; \omega, -\omega)$ are shown in Fig. 4. Unlike the cases for the angular momentum and Peltier effect, in all elements of the conductivity tensor, the resonance peaks appear in the real part of the conductivity. The peaks in $\text{Re}[\Pi^{(L)}]$ for chiral phonons ($\omega \sim 1.47$ and 2.72) show that the orbital current occurs with linearly-polarized light while neither angular momentum nor the Peltier effect occurs. This result is intuitively understandable considering that a linearly polarized light can be viewed as the superposition of right- and left-polarized lights. The right polarized light induces a phonon current with a non-zero phonon angular momentum and the left polarized light induces an opposite phonon current with the opposite angular momentum; the sum of the two results in the orbital current. Indeed, the sign of $\Pi_{\lambda;\mu\nu}^{(L)}$ matches that of the product of $\chi_{\lambda;\mu\nu}^{(L)}$ and $\Pi_{\lambda;\mu\nu}$. The result indicates that chiral phonons can induce a pure orbital current without phonon current and angular momentum.

We note that non-chiral phonons also contributes to the orbital current as in Fig. 4(a). However, in this case, the linearly polarized light also induces orbital angular momentum and Peltier effect; hence, not a pure orbital current. Intuitively, it shows that if a phonon with nonzero angular momentum flows, it also induces an orbital current.

Summary — In this work, we studied the nonlinear responses of chiral phonons to electromagnetic waves:

phonon angular-momentum generation, the Peltier effect of phonons, and the photo-induced phonon orbital current. We find that the angular momentum of the phonon is generated by both chiral and non-chiral phonons. A unique feature of chiral phonons is a polarization-dependent contribution proportional to τ^2 ; this behavior contrasts with the contribution from non-chiral phonons, which is proportional to τ^1 . A similar behavior is also obtained for the Peltier effect of phonons, in which we find a new mechanism unique to the chiral phonons. In addition, we find that the angular momentum and the Peltier effect by chiral phonons are linearly proportional to each other. Lastly, we argued that an orbital photocurrent of phonons, the angular-momentum current similar to the spin current, occurs by the light irradiation. The order estimates of these phenomena indicate that chiral phonons realize larger thermal and orbital responses [35], which facilitates the study of the phenomena and their applications.

This work is supported by JSPS KAKENHI (Grants No. JP23K03275 and JP25H00841), JST PRESTO (Grant No. JPMJPR2452), and JST CREST (Grant No. JPMJCR24R5).

-
- [1] Kyosuke Ishito, Huiling Mao, Yusuke Kousaka, Yoshihiko Togawa, Satoshi Iwasaki, Tiantian Zhang, Shuichi Murakami, Jun-Ichiro Kishine, and Takuya Satoh, “Truly chiral phonons in α -HgS,” *Nature Physics* **19**, 35–39 (2023).
- [2] J. Kishine, A. S. Ovchinnikov, and A. A. Tereshchenko, “Chirality-induced phonon dispersion in a noncentrosymmetric micropolar crystal,” *Phys. Rev. Lett.* **125**, 245302 (2020).
- [3] Hanyu Zhu, Jun Yi, Ming-Yang Li, Jun Xiao, Lifa Zhang, Chih-Wen Yang, Robert A. Kaindl, Lain-Jong Li, Yuan Wang, and Xiang Zhang, “Observation of chiral phonons,” *Science* **359**, 579–582 (2018), <https://www.science.org/doi/pdf/10.1126/science.aar2711>.
- [4] Dominik M. Juraschek, Prineha Narang, and Nicola A. Spaldin, “Phono-magnetic analogs to opto-magnetic effects,” *Phys. Rev. Research* **2**, 043035 (2020), published 7 October 2020.
- [5] Dominik M. Juraschek, Tomáš Neuman, and Prineha Narang, “Giant effective magnetic fields from optically driven chiral phonons in paramagnets,” *Phys. Rev. Research* **4**, 013129 (2022), published 17 February 2022.
- [6] R. Matthias Geilhufe and Wolfram Hergert, “Electron magnetic moment of transient chiral phonons in ktao_3 ,” *Phys. Rev. B* **107**, L020406 (2023), published 18 January 2023.
- [7] Xiaojiang Li, Peisong Peng, Hichem Dammak, Grégory Geneste, Alireza Akbarzadeh, Sergey Prosandeev, L. Bellaiche, and Diyar Talbayev, “Terahertz pulse induced second harmonic generation and kerr effect in the quantum paraelectric,” *Phys. Rev. B* **107**, 064306 (2023), published 21 February 2023.
- [8] M. Basini, M. Pancaldi, B. Wehinger, M. Udina, V. Unnikandanunni, T. Tadano, M. C. Hoffmann, A. V. Balatsky, and S. Bonetti, “Terahertz electric-field-driven dynamical multiferroicity in SrTiO_3 ,” *Nature* **628**, 534–539 (2024), published online 10 April 2024; Issue date: 18 April 2024.
- [9] C. S. Davies, F. G. N. Fennema, A. Tsukamoto, I. Razzol-ski, A. V. Kimel, and A. Kirilyuk, “Phononic switching of magnetization by the ultrafast barnett effect,” *Nature* **628**, 540–544 (2024), published online 10 April 2024; Issue date: 18 April 2024.
- [10] In Hyeok Choi, Seung Gyo Jeong, Sehwan Song, Sungkyun Park, Dong Bin Shin, Woo Seok Choi, and Jong Seok Lee, “Real-time dynamics of angular momentum transfer from spin to acoustic chiral phonon in oxide heterostructures,” (2024).
- [11] D. Lagarde, M. Glazov, V. Jindal, K. Mourzidis, Iann Gerber, A. Balocchi, L. Lombez, P. Renucci, T. Taniguchi, K. Watanabe, C. Robert, and X. Marie, “Efficient electron spin relaxation by chiral phonons in WSe_2 monolayers,” *Phys. Rev. B* **110**, 195403 (2024).
- [12] Tong Lin, Xiaotong Chen, Rui Xu, Jiaming Luo, and Hanyu Zhu, “Ultrafast dynamics of chiral phonons in tungsten disulfide,” in *CLEO 2024* (Optica Publishing Group, 2024) p. FTh5B.5.
- [13] C. Strohm, G. L. J. A. Rikken, and P. Wyder, “Phenomenological evidence for the phonon hall effect,” *Phys. Rev. Lett.* **95**, 155901 (2005).
- [14] L. Sheng, D. N. Sheng, and C. S. Ting, “Theory of the phonon hall effect in paramagnetic dielectrics,” *Phys. Rev. Lett.* **96**, 155901 (2006).
- [15] A. V. Inyushkin and A. N. Taldenkov, “On the phonon hall effect in a paramagnetic dielectric,” *JETP Letters* **86**, 379–382 (2007).
- [16] Yu. Kagan and L. A. Maksimov, “Anomalous hall effect for the phonon heat conductivity in paramagnetic dielectrics,” *Phys. Rev. Lett.* **100**, 145902 (2008).
- [17] Lifa Zhang, Jie Ren, Jian-Sheng Wang, and Baowen Li, “Topological nature of the phonon hall effect,” *Phys. Rev. Lett.* **105**, 225901 (2010).
- [18] Michiyasu Mori, Alexander Spencer-Smith, Oleg P. Sushkov, and Sadamichi Maekawa, “Origin of the phonon hall effect in rare-earth garnets,” *Phys. Rev. Lett.* **113**, 265901 (2014).
- [19] Takuma Saito, Kou Misaki, Hiroaki Ishizuka, and Naoto Nagaosa, “Berry phase of phonons and thermal hall effect in nonmagnetic insulators,” *Phys. Rev. Lett.* **123**, 255901 (2019).
- [20] Xiaouo Zhang, Yinhan Zhang, Satoshi Okamoto, and Di Xiao, “Thermal hall effect induced by magnon-phonon interactions,” *Phys. Rev. Lett.* **123**, 167202 (2019).
- [21] Hiroaki Ishizuka and Naoto Nagaosa, “Local photoexcitation of shift current in noncentrosymmetric systems,” *New Journal of Physics* **19**, 033015 (2017).
- [22] M. Nakamura, S. Horiuchi, F. Kagawa, N. Ogawa, T. Kurumaji, Y. Tokura, and M. Kawasaki, “Shift current photovoltaic effect in a ferroelectric charge-transfer complex,” *Nature Communications* **8**, 281 (2017).
- [23] Takahiro Morimoto, Masao Nakamura, Masashi Kawasaki, and Naoto Nagaosa, “Current-voltage characteristic and shot noise of shift current photovoltaics,” *Phys. Rev. Lett.* **121**, 267401 (2018).
- [24] Hiroki Hatada, Masao Nakamura, Masato Sotome, Yoshio Kaneko, Naoki Ogawa, Takahiro Morimoto, Yoshinori Tokura, and Masashi Kawasaki, “De-

- fect tolerant zero-bias topological photocurrent in a ferroelectric semiconductor,” *Proceedings of the National Academy of Sciences* **117**, 20411–20415 (2020), <https://www.pnas.org/doi/pdf/10.1073/pnas.2007002117>.
- [25] Hiroaki Ishizuka and Naoto Nagaosa, “Theory of bulk photovoltaic effect in anderson insulator,” *Proceedings of the National Academy of Sciences* **118**, e2023642118 (2021), <https://www.pnas.org/doi/pdf/10.1073/pnas.2023642118>.
- [26] Steve M. Young, Fan Zheng, and Andrew M. Rappe, “Prediction of a linear spin bulk photovoltaic effect in antiferromagnets,” *Phys. Rev. Lett.* **110**, 057201 (2013).
- [27] Margarita Davydova, Maksym Serbyn, and Hiroaki Ishizuka, “Symmetry-allowed nonlinear orbital response across the topological phase transition in centrosymmetric materials,” *Phys. Rev. B* **105**, L121407 (2022).
- [28] Igor Proskurin, Alexander S. Ovchinnikov, Jun-ichiro Kishine, and Robert L. Stamps, “Excitation of magnon spin photocurrents in antiferromagnetic insulators,” *Phys. Rev. B* **98**, 134422 (2018).
- [29] Hiroaki Ishizuka and Masahiro Sato, “Theory for shift current of bosons: Photogalvanic spin current in ferrimagnetic and antiferromagnetic insulators,” *Phys. Rev. B* **100**, 224411 (2019).
- [30] Hiroaki Ishizuka and Masahiro Sato, “Rectification of spin current in inversion-asymmetric magnets with linearly polarized electromagnetic waves,” *Phys. Rev. Lett.* **122**, 197702 (2019).
- [31] Hiroaki Ishizuka and Masahiro Sato, “Large photogalvanic spin current by magnetic resonance in bilayer or trihalides,” *Phys. Rev. Lett.* **129**, 107201 (2022).
- [32] Kosuke Fujiwara and Takahiro Morimoto, “Interaction-induced nonlinear magnon transport in noncentrosymmetric magnets,” *Phys. Rev. B* **111**, 014408 (2025).
- [33] Hiroaki Ishizuka and Masahiro Sato, “Peltier effect of phonons driven by electromagnetic waves,” *Phys. Rev. B* **110**, L020303 (2024).
- [34] Hirokazu Tsunetsugu and Hiroaki Kusunose, “Theory of energy dispersion of chiral phonons,” *Journal of the Physical Society of Japan* **92**, 023601 (2023), <https://doi.org/10.7566/JPSJ.92.023601>.
- [35] Hiroaki Ishizuka and Masahiro Sato, “Supplemental material for “nonlinear optical response of truly chiral phonons: Light-induced phonon angular momentum, peltier effect, and orbital current”,” <https://xxxxx> (2025), published as supplemental material to xxxx.
- [36] I. Božović, “Possible band-structure shapes of quasi-one-dimensional solids,” *Physical Review B* **29**, 6586–6599 (1984).
- [37] Lifa Zhang and Qian Niu, “Angular momentum of phonons and the einstein–de haas effect,” *Phys. Rev. Lett.* **112**, 085503 (2014).
- [38] H. Chen, W. Zhang, Q. Niu, and L. Zhang, “Chiral phonons in two-dimensional materials,” *2D Materials* **6**, 012002 (2019).
- [39] Robert J. Hardy, “Energy-flux operator for a lattice,” *Phys. Rev.* **132**, 168–177 (1963).
- [40] Ralph von Baltz and Wolfgang Kraut, “Theory of the bulk photovoltaic effect in pure crystals,” *Phys. Rev. B* **23**, 5590–5596 (1981).
- [41] J. E. Sipe and A. I. Shkrebtii, “Second-order optical response in semiconductors,” *Phys. Rev. B* **61**, 5337–5352 (2000).